USE OF SAMPLING FEEDBACK SYSTEM FOR STABILIZATION OF LOW FREQUENCY OSCILLATIONS IN LIQUID MONOPROPELLANT ROCKET MOTORS

C. FERNÁNDEZ, JR.

A-53

USE OF A SAMPLING FEEDBACK SYSTEM FOR STABILIZATION OF LOW FREQUENCY OSCILLATIONS IN LIQUID MONOPROPELLANT ROCKET MOTORS

Thesis by

LCDR C. Fernández, Jr., USN

In Partial Fulfillment of the Requirements

For the Degree of

Aeronautical Engineer

California Institute of Technology

Pasadena, California

1953

F26

ACKNOWLEDGEMENT

The author is deeply grateful to Dr. Frank E. Marble, of the Daniel and Florence Guggenheim Jet Propulsion Center, California Institute of Technology, for help and guidance in this problem.

The author wishes to thank Mrs. Virginia Boughton for typing the thesis.

ABSTRACT

Instability in liquid monopropellant rocket motors may be corrected by the use of a feedback servomechanism. This mechanism consists essentially of a pressure pickup which senses pressure oscillations in the combustion chamber, an amplifier and a variable capacitance in the feed line. It is shown that a feedback system with an arbitrary sampling circuit which causes the capacitance in the line to complete its own cycle of variation once for every several cycles of combustion pressure oscillations can be made to stabilize the oscillations for all values of combustion time lag for a particular motor. It is believed that this system of stabilization may be applied to monopropellant motors in general.

TABLE OF CONTENTS

SYMBOLS AND DEFINITIONS

t = time

τ = time lag

p = instantaneous value of pressure

n = dimensionless quantity relating pressure and time lag

$\bar{p}$ = steady-state pressure in the combustion chamber

$\Delta\bar{p}$ = injector pressure drop

P = $\bar{p}/2\Delta\bar{p}$, injector pressure drop parameter

l = distance along feed line between pump outlet and injector

$\bar{\dot{m}}$ = steady-state mass flow rate

A = cross-sectional area of the feed line

θ_g = gas residence time in the combustion chamber

J = $l\bar{\dot{m}}/2\Delta\bar{p}A\theta_g$ line inertia characteristic parameter

p_o = instantaneous value of pump outlet pressure

$\bar{p}_o$ = steady-state value of pump outlet pressure

$\dot{m}_o$ = instantaneous value of pump outlet mass flow rate

α = $-\bar{\dot{m}}(p_o-\bar{p})/\bar{p}_o(\dot{m}_i-\bar{\dot{m}})$ pump delivery characteristic parameter

ϕ = $(p-\bar{p})/\bar{p}$, fractional variation of pressure in the combustion chamber

z = t/θ_g , reduced time

δ = τ/θ_g , reduced time lag

μ = $(\dot{m}_i-\bar{\dot{m}})/\bar{\dot{m}}$ fractional variation in injector mass flow rate

λ = reduced amplification coefficient

ω = reduced angular frequency (real frequency divided by residence time)

s = $\lambda + i\omega$

$\kappa(z)$ = instantaneous value of capacitance

$F_1(z)$ = transfer function of sampling circuit

$F_2(z)$ = transfer function of amplifier

I. INTRODUCTION

The low frequency, "chugging", oscillations in liquid rocket motors have been attributed to the coupled effects of the feed system and combustion chamber dynamics. According to D. F. Gunder and D. R. Friant[1], the pressure oscillations can take place in the combustion chamber merely as a result of small changes in the velocity of flow in the injected fuel; that is, if for any reason the flow rate decreases, the rate of burning and hence the pressure will decrease a short time later in the chamber. Then, as the pressure drop is felt at the injector the flow rate will increase and a short time later the pressure at the point of combustion will increase resulting finally in a decrease in rate of flow from the injection nozzle, the cycle continuing indefinitely. The explanation for this phenomenon involves the concepts of time lag between the instant of injection and transformation of the fuel to hot combustion products, and of the dependence of the rate of burning on combustion chamber pressure.

M. Summerfield[2] has shown how the length of feed line, the velocity of the propellant in the feed line, the ratio of feed pressure to chamber pressure and the ratio of chamber volume to nozzle area affect chugging oscillations and has discussed the trend of changes required in the feed system and motor parameters to suppress these oscillations.

L. Crocco[3] has introduced the concept of variable time lag basing this concept on a qualitative analysis of the complicated processes that affect the propellants from the time of injection to the

time of burning. He has formulated a relation between time lag and pressure showing that if the pressure is oscillating, the time lag is also an oscillating quantity around an average value. Using this idea he has demonstrated that self-excited oscillations in the combustion chamber can exist even in the absence of any variation in the injection rate. In the case where the time lag is decreasing the burning of the particles that were injected later catch up with the burning of those that were injected earlier and an increase in rate of burning would result, the opposite being true if the time lag were increasing; then, if the variations in time lag coincided with the variations in pressure in a certain manner, self-excited oscillations would be produced.

H. S. Tsien[4] has demonstrated that a feedback servomechanism may be used to stabilize combustion chamber pressure oscillations for all values of time lag, thus making it possible to stabilize motors for which a change in configuration parameters alone would not correct instability or where such changes would not be feasible. The servomechanism Tsien proposed consists essentially of a feedback servocontrol which senses the oscillating pressure in the combustion chamber and changes the propellant flow by the proper amount and in the proper phase to damp the oscillations. Such a system is shown schematically on Figure 1.

A servomechanism in which the variable capacitance is required to oscillate at the same frequency as the chamber pressure fluctuations is likely to produce at least two important problems

arising from the rate at which these oscillations generally occur, namely in the order of 100 per second. One is the difficulty of producing sizeable changes in capacitance at such frequencies, and the other is cavitation in the fluid. If the variable capacitance consists of a piston-cylinder mechanism, it would help to lessen the problems to move the piston down on the compression stroke at the same frequency as the chamber oscillation and to withdraw the piston slowly to the maximum-capacity position in the time required for several pressure oscillations in the chamber to take place. With the proper phasing and amplitude it should be possible to damp out pressure oscillations in the chamber.

The purpose of this investigation is to design a feedback circuit that will detect symmetric (say sinusoidal) oscillations in the combustion chamber and provide signals to the servomotor that will produce the asymmetric motion described above and provide stability for all values of combustion time lag.

As an extension of Tsien's work, F. E. Marble and D. W. Cox[5] have shown that a feedback servomechanism may stabilize liquid bipropellant motors as well as monopropellant motors. Their general method for designing the stabilizing transfer function of the feedback loop will be used in this investigation.

II. DYNAMICS OF THE MONOPROPELLANT MOTOR

The basic motor without feedback control considered in this investigation essentially consists of a combustion chamber, injector, feed line and fuel pump. It may be thought of as two dynamic systems: one, the combustion chamber and the discharge nozzle; the other, the propellant supply system consisting of the propellant pump, propellant line and injector. These two systems are coupled through the requirement that the mass of propellant discharged from the propellant line appear in the combustion chamber. The performance of the combustion chamber is characterized by a mean pressure $\bar{p}$, a mean residence time θ_g and a mean flow rate $\bar{\dot{m}}$. When the chamber pressure varies from p its fractional variation will be denoted $\phi = \frac{p - \bar{p}}{\bar{p}}$. The performance of the propellant feed system depends upon the cross-sectional area A and length ℓ of the feed line, the pressure drop $\Delta\bar{p}$ across the injector and the local slope α of the mass flow-pressure characteristics of the pump where $\alpha = -\frac{\dot{m}_o - \bar{\dot{m}}_o}{\bar{\dot{m}}_o} \frac{\bar{p}_o}{p_o - \bar{p}_o}$. The fractional variation in propellant injection rate will be defined as $\mu = \frac{\dot{m}_i - \bar{\dot{m}}}{\bar{\dot{m}}}$.

The fuel injected into the chamber does not burn immediately but only after it has remained a certain time τ in the chamber. The time τ required for the transformation of propellant into products of combustion may be represented by means of the integral

$$\int_{t-\tau}^{t} f(\bar{p}, \bar{T}_g) \qquad = \text{constant}$$

where $f(p, T_g)$ is a function depending upon the mechanics of the

process, and T_g is the ambient gas temperature in the neighborhood of the injector. Since the time lag τ depends upon the chamber pressure it varies with time in the same manner as the chamber pressure does. In fact Tsien[4] has shown that

$$\frac{d\tau}{dt} = n \frac{p(t-\tau) - p(\tau)}{\bar{p}}$$

where

$$n = \frac{\partial \log f(\bar{p}, \bar{T}_g)}{\partial \log \bar{p}}$$

Now, as shown by Crocco[3], the continuity of mass flow through the combustion chamber may be written as

$$\frac{d\phi}{dz} + (1-n)\phi(z) + n\phi(z-\delta) - \mu(z-\delta) = 0 \qquad (1)$$

where δ is the reduced time lag $\frac{\tau}{\theta_g}$ and $z = \frac{t}{\theta_g}$. Furthermore, defining

$$P = \frac{\bar{p}}{2\Delta\bar{p}} \qquad J = \frac{\rho \bar{\dot{m}}}{2\Delta\bar{p} A \theta_g}$$

the dynamic equilibrium of the propellant supply system is given by

$$J\frac{d\mu}{dz} + \left[\frac{1}{2}\left(P + \frac{1}{2}\right) + 1\right]\mu + P\phi = 0 \qquad (2)$$

The presence of ϕ and μ in Equations (1) and (2) indicates the coupling between the chamber and feed systems.

To analyze the stability of the system the following solutions may be tried:

$$\phi(z) = \Phi(s)e^{sz}, \quad \phi(s-z) = \Phi(s)e^{(s-\delta)z}, \quad \mu(z) = M(s)e^{sz}$$

where $s = \lambda + i\omega$. Using these trial solutions and eliminating the common factor e^{sz} Equations (1) and (2) represent a solution of the system if the two homogeneous equations below are simultaneously satisfied:

$$(s+1-n+ne^{-s\delta})\Phi(s) - e^{-s\delta} M(s) = 0 \qquad (3)$$

$$P\Phi(s) + \left[Js + \frac{1}{a}(P+\frac{1}{2}) + 1\right] M(s) = 0 \qquad (4)$$

For non-trivial solutions the determinant of the coefficients of Equations (3) and (4) must vanish, that is

$$\begin{vmatrix} s+1-n+ne^{-s\delta} & -e^{-s\delta} \\ P & Js + \frac{1}{a}(P+\frac{1}{2})+1 \end{vmatrix} \equiv G'(s) = 0 \qquad (5)$$

This is a transcendental equation in the complex variable s , the roots of which determine the stability of pressure oscillations. If any root of $G'(s)=0$ possesses a positive real part the system is unstable. The Nyquist criterion may be applied to $G'(s)$ to determine the existence of such roots [5]. In this method the variable s traces a contour enclosing the right-half complex plane. As s moves in the manner shown in Figure 2, that is, along the imaginary axis and a large half circle to the right, the behavior of $G'(s)$ is plotted and the number of complete revolutions noted. This number

is the difference between the number of roots and poles of $G'(s)$ in the right half s-plane. If the number of poles can be determined independently the number of roots is known and the stability determined.

The term $e^{-s\delta}$ in $G'(s)$ makes use of the Nyquist diagram difficult. A complete investigation would require plotting the function $G'(s)$ for many values of δ, the reduced time lag. A different technique, proposed by M. Satche[6] and developed by Tsien[4], requires the function $G'(s)$ to be separated into two parts, the first consisting only of $e^{-s\delta}$ and the second of the remaining terms. In this case $G'(s)$ may be expressed as a combination of two determinants

$$\mathfrak{D}_1(s) = \begin{vmatrix} s+1-n & 0 \\ P & Js + \frac{1}{\alpha}(P+\frac{1}{2}) + 1 \end{vmatrix} \tag{6}$$

$$\mathfrak{D}_2(s) = \begin{vmatrix} n & -1 \\ P & Js + \frac{1}{2}(P+\frac{1}{2}) \end{vmatrix} \tag{7}$$

so that Equation (5) may be written

$$\mathfrak{D}_1(s) + e^{-s\delta}\mathfrak{D}_2(s) = 0 \tag{8}$$

Following Tsien[4] in calling $e^{-s\delta} \equiv g_1(s)$ and $\frac{\mathfrak{D}_1(s)}{\mathfrak{D}_2(s)} \equiv -g_2(s)$, Equation (8) becomes

$$g_1(s) - g_2(s) \equiv G(s) \tag{9}$$

and $g_1(s)$ and $g_2(s)$ may be plotted separately. For neutral stability $Re(s) = 0$ and $g_1(i\omega)$ becomes a unit circle on the Satche diagram; all unstable roots lie within the unit circle. Assuming that $G(s)$

has no poles in the right-half plane then if $g_2(s)$ either passes through the unit circle or encircles the origin the system is unstable, while the converse is true. The function G(s), however, may have poles in the right-half plane because of possible zeros in the denominator determinant $D_2(s)$. This number of poles may be found by applying the Nyquist criterion to $D_2(s)$ and this number must be added to whatever number of turns $g_2(s)$ makes about the origin.

As an example of the above criteria applied to a specific case a motor with the following parameters may be considered:

$$\alpha = 1.0 \qquad J = 1.5 \qquad n = 0.6 \qquad P = 1.0$$

Expressing $D_1(s)$ and $D_2(s)$ as follows:

$$D_1(s) \equiv d_1^{(0)} + d_1^{(1)} s + d_1^{(2)} s^2 \tag{10}$$

$$D_2(s) \equiv d_2^{(0)} + d_2^{(1)} s \tag{11}$$

the coefficients become:

$$d_1^{(0)} = \left[1 + \frac{1}{\alpha}\left(P + \tfrac{1}{2}\right)\right](1-n) \qquad d_2^{(0)} = P + n\left[1 + \frac{1}{\alpha}\left(P + \tfrac{1}{2}\right)\right]$$

$$d_1^{(1)} = \left[J(1-n) + 1 + \frac{1}{\alpha}\left(P + \tfrac{1}{2}\right)\right] \qquad d_2^{(1)} = nJ \tag{12}$$

$$d_1^{(2)} = J$$

For this particular motor

$$d_1^{(0)} = 1 \qquad d_2^{(0)} = 2.5$$

$$d_1^{(1)} = 3.1 \qquad d_2^{(1)} = 0.9$$

$$d_1^{(2)} = 1.5$$

The characteristic equation for s is

$$e^{-s\delta} + \frac{1 + 3.1\,s + 1.5\,s^2}{2.5 + 0.9\,s} = 0$$

For the case where $s = i\omega$, along the imaginary axis,

$$g_2(i\omega) = -\frac{1 + 3.1\,i\omega - 1.5\,\omega^2}{2.5 + 0.9\,i\omega}$$

$$= \frac{0.96\omega^2 - 2.5}{6.25 + 0.81\,\omega} - \frac{1.35\,\omega^3 - 6.85}{6.25 + 0.81\,\omega}\,i$$

The Satche diagram for this function is shown on Figure 3. The function $g_2(i\omega)$ crosses the unit circle and indicates instability for values of ω below approximately 0.9. For large values of s off the imaginary axis, let $s = Re^{i\theta}$. Then $g_2(s)$ behaves as $-Re^{i\theta}$ and as θ decreases from $\pi/2$ to $-\pi/2$ the curve progresses clockwise in a large arc from $-\infty i$ to $+\infty i$ in the left-half plane without encircling the origin indicating no further instability.

References 4 and 5 contain examples of stable and unstable motor behavior as determined by analyses similar to the above.

III. FEEDBACK STABILIZATION

The unstable operation of a motor with fixed parameters may be corrected by means of a simple feedback servomechanism, consisting of a combustion chamber pressure pickup instrument, sampling circuit, amplifier, servomotor and a variable capacitance. A feedback system in a stability analysis provides a mathematical relation between the combustion chamber pressure and the variable capacitance and introduces a new coupling term in the relations for the simple circuit without feedback. The relation between the capacitance $K(z)$ and the pressure may be written symbolically as

$$K(z) = F_2 \frac{d}{dz} \left[F_1 \frac{d}{dz} \phi(z) \right]$$

where $F_2 \frac{d}{dz}$ and $F_1 \frac{d}{dz}$ are linear differential-integral operators of the amplifier and sampling circuit, respectively. The above relation indicates that the line capacitance changes with time in accordance with the amplifier signals whose action is controlled by a sampling circuit, which interprets the combustion chamber pressure impulses in a certain manner.

A new set of simultaneous differential equations arises from the introduction of the feedback loop [5]:

$$\frac{d\phi}{dz} + (1-n)\phi + n\phi(z-\delta) - \mu(z-\delta) = 0$$

$$J\frac{d\mu}{dz} + \left[\frac{1}{\alpha}\left(P+\frac{1}{2}\right)+1\right]\mu + P\phi + J\frac{d^2K(z)}{dz^2} + \frac{1}{\alpha}\left(P+\frac{1}{2}\right)\frac{dK(z)}{dz} = 0$$

$$F_2 \frac{d}{dz}\left[F_1 \frac{d}{dz}\phi(z)\right] - K(z) = 0$$

Using trial solutions

$$K(z)=K(s)\,e^{sz}, \qquad \phi(z)=\Phi(s)\,e^{sz}, \qquad \mu(z)=M(s)\,e^{sz}.$$

a set of homogeneous simultaneous equations similar to (3) and (4) is obtained,

$$(s+1-n+ne^{-s\delta})\,\Phi(s)-e^{-s\delta}M(s)=0$$

$$P\Phi(s)+\left[Js+\tfrac{1}{\alpha}(P+\tfrac{1}{2})+1\right]M(s)+\left[Js^2+\tfrac{1}{\alpha}(P+\tfrac{1}{2})s\right]K(s)=0$$

$$F_1(s)\,F_2(s)\,\Phi(s)-K(s)=0$$

where $F_1(s)$ and $F_2(s)$ are the transfer functions of the sampling circuit and the amplifier circuit, respectively. The stability of the system now depends on the roots of the third order determinant, formed from the coefficients of the above set of equations

$$\begin{vmatrix} s+1-n+ne^{-s\delta} & -e^{-s\delta} & 0 \\ P & Js+1+\frac{1}{\alpha}(P+\frac{1}{2}) & Js^2+\frac{1}{\alpha}(P+\frac{1}{\alpha})s \\ F_1(s)\,F_2(s) & 0 & -1 \end{vmatrix} \qquad (13)$$

This determinant may be conveniently expressed in terms of $\mathcal{D}_1(s)$, Equation (6), $\mathcal{D}_2(s)$ Equation (7), and a third minor defined as $\mathcal{D}_f(s)$

$$\mathcal{D}_f(s) \equiv \begin{vmatrix} 1 & 0 \\ Js+1+\frac{1}{\alpha}(P+\frac{1}{2}) & Js^2+\frac{1}{\alpha}(P+\frac{1}{2}) \end{vmatrix} \qquad (14)$$

The new characteristic equation obtained by setting the stability determinant (13) equal to zero is

$$\mathcal{D}_1(s)+e^{-s\delta}\left[\mathcal{D}_2(s)+F_1(s)\,F_2(s)\,\mathcal{D}_f(s)\right]=0 \qquad (15)$$

For stability analysis using the Satche diagram Equation (15) may

be written

$$e^{-s\delta} + \frac{\mathfrak{D}_1(s)}{\mathfrak{D}_2(s) + F_1(s)\, F_2(s)\, \mathfrak{D}_4(s)} = 0 \qquad (16)$$

where $g_1(s)$ and $g_2(s)$ now correspond to the first and second terms, respectively, of the above equation and may be plotted separately on the Satche diagram. Stable motor operation is to be assured by choosing the form of $F_1(s)$ and $F_2(s)$ so that the stability criteria are satisfied. It should be noted that $\mathfrak{D}_1(s)$, $\mathfrak{D}_2(s)$ and $\mathfrak{D}_4(s)$ are functions of the fixed motor parameters and are independent of the feedback functions.

Generally, instability in the basic motor arises from the intersection of the $g_2(i\omega)$ curve with the unit circle as in Figure 3, where the reduced angular frequency is in the order of unity at the point of intersection. If for higher frequencies the function $g_2(s)$ shows no further instability as is generally the case it is necessary only to modify $g_2(i\omega)$ to move clear of the unit circle for small values of ω and to cause the gain of the amplifier to disappear at higher frequencies.

IV. SAMPLING CIRCUIT FOR FEEDBACK SYSTEM

The functions of the feedback circuit in this investigation will be divided into two parts: one, to provide stabilization and control the gain at different frequencies and the other, to transform the pressure signal received from the combustion chamber in such a manner that the compression stroke of the variable-capacitance will be of the same frequency and the return stroke will take considerably longer time. A sampling circuit will be responsible for carrying out this latter task while the stabilizing function will be carried out by the amplifier.

As a representative example, let the pressure signals received by the sampling circuit from the combustion chamber be sinusoidal, and the signals which the sampling circuit delivers to the amplifier be represented by an asymmetric function, as follows:

Into the sampling circuit

$$\sin z$$

Out of the sampling circuit

$$f(z) \begin{cases} = \cos z & \text{interval} \quad 0 \leq z \leq \pi \\ = -\cos \dfrac{z-\pi}{2q-1} & \text{interval} \quad \pi \leq z \leq 2\pi q \end{cases}$$

The input and output functions are shown graphically on Figure 4. Over a total interval of time $2\pi q$ there are q pressure cycles in the combustion chamber for each cycle of motion in the variable capacitance.

The function $f(z)$ may be expanded in a Fourier series

$$f(z) = \sum_{k=1}^{\infty} \left(a_k \cos \frac{k}{q} z + b_k \sin \frac{k}{q} z\right)$$

The coefficients are

$$a_k = \frac{1}{\pi q} \int_0^{2\pi q} f(z) \cos \frac{k}{q} z \, dz$$

$$b_k = \frac{1}{\pi q} \int_0^{2\pi q} f(z) \cos \frac{k}{q} z \, dz$$

Replacing f(z) by the required output functions in the above equations the following general expressions for the coefficients are obtained

$$a_k = \frac{1}{\pi q} \int_0^{\pi} \cos z \cos \frac{k}{q} z \, dz - \frac{1}{\pi q} \int_0^{2\pi q} \cos \frac{z-\pi}{2q-1} \cos \frac{k}{q} z \, dz$$

$$= \frac{k}{\pi} \sin \frac{k}{q} \pi \left[\frac{1}{q^2 + k^2} - \frac{1}{\frac{q^2}{(2q-1)^2} - k^2} \right]$$

$$b_k = \frac{1}{\pi q} \int_0^{\pi} \cos z \sin \frac{k}{q} z \, dz - \frac{1}{\pi q} \int_0^{2\pi q} \cos \frac{z-\pi}{2q-1} \sin \frac{k}{q} z \, dz$$

$$= \frac{k}{\pi} \left[\frac{1 + \cos \frac{k}{q} \pi}{\frac{q^2}{(2q-1)^2} - k^2} - \frac{\cos \frac{k}{q} \pi}{q^2 - k^2} \right]$$

The second expressions for a_k and b_k above may be used to evaluate the coefficients when $q \neq k$. For the case where $q = k$ the integral expressions used directly are more convenient.

Anticipating the use of an illustrative example the coefficients for the first eight terms of the Fourier series using a value of $q = 4$ have been calculated and are tabulated below.

k	a_k	b_k
1	0.350	-0.821
2	0.226	-0.1731
3	0.174	0.0643
4	0.125	0
5	0.0794	-0.144
6	0.0420	-0.0535
7	0.0154	-0.0303
8	0	-0.027

Now, it is necessary to obtain the transfer function of this sampling circuit in terms of the complex variable s eventually to investigate the stability of the system. The transfer function is the ratio of the Laplace transforms of the output and input functions of the sampling circuit.

The Laplace transform of the output function is

$$\int_0^\infty f(z)e^{-sz}\,dz = \int_0^\infty \sum_{k=1}^{\infty} \left(a_k \cos\frac{k}{q}z + b_k \sin\frac{k}{q}z\right) e^{-sz}\,dz$$

$$= \sum_{k=1}^{\infty} a_k \frac{s}{s^2+\frac{k^2}{q^2}} + \sum_{k=1}^{\infty} b_k \frac{\frac{k}{q}}{s^2+\frac{k^2}{q^2}} = \sum_{k=1}^{\infty} \frac{q}{s^2q^2+k^2}(a_k q s + b_k k)$$

Similarly for the input circuit

$$\int_0^\infty \sin z\, e^{-sz}\,dz = \frac{1}{s^2+1}$$

Therefore, the transfer function of the sampling circuit may be written as

$$F_1(s) = \sum_{k=1}^{\infty} \frac{s^2 + 1}{q\left(s^2 + \frac{k^2}{q^2}\right)} \left(a_k q s + b_k k\right) \qquad (17)$$

Introducing a term $2cs$ in (17) to take into account the damping which exists in a real circuit because of resistance elements the function $F_1(s)$ will be modified as follows:

$$F_1(s)_{,\,modified} = \sum_{k=1}^{\infty} \frac{1}{q} \frac{1 + 2cs + s^2}{\frac{k^2}{q^2} + 2cs + s^2} \left(a_k q s + b_k s\right) \qquad (18)$$

It is now possible to proceed to the development of the appropriate amplifier transfer function and to determine the overall stability of the system.

V. AMPLIFIER CHARACTERISTICS AND STABILITY ANALYSIS

An appropriate procedure for determining the amplifier characteristics is[5], (1) to find the approximate behavior of $F_2(s)$ for $s=i\omega \ll i$ such that $g_2(i\omega)$ does not intersect the unit circle and (2) to determine the function $F_2(s)$ so that it has the prescribed behavior for small values of ω and vanish for large ω. The first part of the procedure may be carried out in the following manner. Each of the terms in the expression for $g_2(s)$,

$$g_2(s) = -\frac{\mathfrak{D}_1(s)}{\mathfrak{D}_2(s) + F_1(s) F_2(s)\, \mathfrak{D}_f(s)} \tag{19}$$

obtained from Equation (16) may be expressed as a power series in . Thus

$$\mathfrak{D}_1(s) = d_1^{(0)} + d_1^{(1)} s + d_1^{(2)} s^2$$

$$\mathfrak{D}_2(s) = d_2^{(0)} + d_2^{(1)} s$$

and
$$\mathfrak{D}_f(s) = B_1 s + B_2 s^2 \tag{20}$$

where
$$B_1 = \frac{1}{\alpha}\left(P + \frac{1}{2}\right), \quad B_2 = J \tag{21}$$

The B_i are obtained by expanding the determinant of Equation (14). The terms $\mathfrak{D}_1(s)$, $\mathfrak{D}_2(s)$ and $\mathfrak{D}_f(s)$ depend only on the fixed parameters of the basic motor. Equation (18) representing the transfer function $F_1(s)$ of the sampling circuit may be expanded as follows

$$F_1(s) = \sum_{k=1}^{\infty} \frac{q b_k}{k} \frac{(1 + 2cs + s^2)\left(1 + \frac{a_k q}{b_k k} s\right)}{1 + \frac{q^2}{k^2}(2cs + s^2)}$$

$$\cong \sum_{k=1}^{\infty} \frac{q b_k}{k} (1+2cs+s^2)\left[1 - \frac{q^2}{k^2}(2cs+s^2) + \frac{q^4}{k^4}(2cs+s^2)^2 + \cdots\right]\left(1 + \frac{a_k q}{b_k k} s\right)$$

$$\cong \sum_{k=1}^{\infty} \frac{qb_k}{k} + \sum_{k=1}^{\infty} \frac{qb_k}{k} \left[2c\left(1 - \frac{q^2}{k^2}\right) + \frac{a_k q}{b_k k} \right] s$$

$$+ \sum_{k=1}^{\infty} \frac{qb_k}{k} \left\{ 1 + 2c \frac{q}{k} \left[\frac{a_k}{b_k} - \frac{q}{k}\left(2c + \frac{a_k q}{b_k k}\right)\right] - \frac{q^2}{k^2}\left(1 - 4c^2 \frac{q^2}{k^2}\right) \right\} s^2 + \cdots \qquad (22)$$

It is appropriate to choose the following form for the amplifier transfer function

$$F_2(s) \cong f_2^{(-1)} \frac{1}{s} + f_2^{(0)} + f_2^{(1)} s \qquad (23)$$

where the f_2^i are unknown constants. The function $g_2(s)$ may now be written

$$g_2(s) \cong \frac{-\left(d_1^{(0)} + d_1^{(1)} s + d_1^{(2)} s^2\right)}{d_2^{(0)} + d_2^{(1)} s + \left(A_0 + A_1 s + A_2 s^2\right)\left(\frac{f_2^{(-1)}}{s} + f_2^{(0)} + f_2^{(1)} s\right)\left(B_1 s + B_2 s^2\right)} \qquad (24)$$

where, for brevity, A_i represent the coefficients of s in the approximate expression for $F_1(s)$, Equation (22). The reason for choosing the form for $F_2(s)$ of Equation (23) becomes clear from inspection of Equation (24), since, for $s = 0$

$$g_2(0) = \frac{-d_1^{(0)}}{d_2^{(0)} + A_0 f_2^{(-1)} B_1}$$

and $g_2(0)$ remains finite. Now the requirement that the curve lie outside the unit circle for small ω may be met as follows. Prescribe $g_2(i\omega)$ by the polynomial

$$g_2(i\omega) = \gamma_0 + \gamma_1 (i\omega) + \gamma_2 (i\omega)^2 \qquad (25)$$

choosing the γ_i so that stability will be obtained. Then there are

two expressions for $g_2(s)$ valid for small s, namely

$$g_2(s) = \gamma_0 + \gamma_1 s + \gamma_2 s^2 \tag{26}$$

and Equation (24). Since these two expressions are power series expansions in s they are equal term by term. The results of setting coefficients of like powers of s equal to each other are expressions relating the unknown constants f_2^i and the known coefficients from which the values of f_2^i may be calculated. Thus, after performing the necessary operations and retaining terms in s of no higher power than s^2 the following expressions for the f_2^i are obtained:

$$f_2^{(-1)} = \frac{1}{B_1 \sum_{k=1}^{\infty} \frac{qb_k}{k}} \left(-\frac{d_1^{(0)}}{\gamma_0} - d_2^{(0)} \right) \tag{27}$$

$$f_2^{(0)} = \frac{1}{B_1 \sum_{k=1}^{\infty} \frac{qb_k}{k}} \left\{ -\frac{d_1^{(1)}}{\gamma_0} - \frac{\gamma_1}{\gamma_0} \left(B_1 \sum_{k=1}^{\infty} \frac{qb_k}{k} + d_2^{(0)} \right) \right. \tag{28}$$

$$\left. - B_1 \sum_{k=1}^{\infty} \frac{qb_k}{k} f_2^{(-1)} \left[2c \left(1 - \frac{q^2}{k^2} \right) + \frac{a_k q}{b_k k} \right] - B_2 \sum_{k=1}^{\infty} \frac{qb_k}{k} f_2^{(-1)} - d_2^{(1)} \right\}$$

$$f_2^{(1)} = \frac{1}{B_1 \sum_{k=1}^{\infty} \frac{qb_k}{k}} \left\{ -\frac{d_1^{(2)}}{\gamma_0} - B_1 \sum_{k=1}^{\infty} \frac{qb_k}{k} \left[f_2^{(-1)} \left\{ 1 + 2c \frac{q}{k} \left[\frac{a_k}{b_k} - \frac{q}{k} \left(2c + \frac{a_k q}{b_k k} \right) \right] - \frac{q^2}{k^2} \left(1 - 4c^2 \frac{q^2}{k^2} \right) \right\} \right. \right.$$

$$\left. + f_2^{(0)} \left[2c \left(1 - \frac{q^2}{k^2} \right) + \frac{a_k q}{b_k k} \right] \right]$$

$$- B_2 \sum_{k=1}^{\infty} \frac{qb_k}{k} \left\{ f_2^{(-1)} \left[2c \left(1 - \frac{q^2}{k^2} \right) + \frac{a_k q}{b_k k} \right] + f_2^{(0)} \right\}$$

$$\left. - \frac{\gamma_1}{\gamma_0} \left[B_1 \sum_{k=1}^{\infty} \frac{qb_k}{k} \left\{ f_2^{(-1)} \left[2c \left(1 - \frac{q^2}{k^2} \right) + \frac{a_k q}{b_k k} \right] + f_2^{(0)} \right\} + B_2 \sum_{k=1}^{\infty} \frac{qb_k}{k} f_2^{(-1)} + d_2^{(1)} \right] \right.$$

$$\left. - \frac{\gamma_2}{\gamma_0} \left(B_1 \sum_{k=1}^{\infty} \frac{qb_k}{k} f_2^{(-1)} + d_2^{(0)} \right) \right\} \tag{29}$$

The second part of the procedure for determining the complete amplifier transfer function is to obtain an expression which agrees with Equation (23) for small values of s and will vanish for large values of s so as to leave the original Satche diagram unchanged for large s. Consider the following choice of $F_2(s)$

$$F_2(s) = \frac{f_2^{(-1)}}{s}\left(\frac{1 + as + bs^2}{1 + hs^4}\right) \tag{30}$$

where a, b, and h are constants. For small values of s

$$F_2(s) \cong \frac{f_2^{(-1)}}{s}\,(1 + as + bs^2)$$

and the coefficients a and b must become

$$a = \frac{f_2^{(0)}}{f_2^{(-1)}}, \qquad b = \frac{f_2^{(1)}}{f_2^{(-1)}} \tag{31}$$

in order that $F_2(s)$ may agree with Equation (23). For large s, $F_2(s)$ will behave as $\frac{1}{hs^3}$, causing the second term in the denominator of $g_2(s)$ in Equation (19), that is, the product $F_1(s)\,F_2(s)\,D_f(s)$, to behave as s^0 so that the value of $g_2(s)$ becomes nearly that of the basic motor without feedback. The value of h must be such that stability will be obtained for all values of s and will be determined largely by trial and error.

The exact expression for the function $g_2(s)$ becomes then, for all values of s

$$g_2(s) = \frac{-\left(d_1^{(0)} + d_1^{(1)}s + d_1^{(2)}s^2\right)}{d_1^{(0)} + d_1^{(1)}s + \sum_{k=1}^{\infty}\frac{(1+2cs+s^2)(qa_k s + kb_k)}{\frac{k^2}{q^2} + 2cs + s^2}\,\frac{f_2^{(-1)}}{s}\,\frac{(1+0s+bs^2)}{1+hs^4}\left(B_1 s + B_2 s^2\right)} \tag{32}$$

To illustrate the application of the stabilization procedure consider the unstable motor for which the Satche diagram is shown on Figure 3. To provide stabilization at low values of ω the curve of $g_2(i\omega)$ must be moved away from unit circle. Choosing the following values of γ_i

$$\gamma_0 = -1.25 \quad , \quad \gamma_1 = -2.0 \quad , \quad \gamma_2 = -0.25$$

and using Equation (25) for $g_2(i\omega)$ the dashed line on Figure 3 is obtained. From Equations (27), (28) and (29), using a value of $c = 0.1$, and summing over the first eight terms of the Fourier coefficients, the f_2^i are

$$f_2^{(-1)} = 0.304 \quad , \quad f_2^{(0)} = 0.032 \quad , \quad f_2^{(1)} = 5.34 \quad ,$$

which fixes the feedback loop for small values of ω . To obtain the general expression for the amplifier transfer function the constants a and b are, from Equations (31),

$$a = 3.395 \qquad b = 17.48$$

and $F_2(s)$ becomes

$$F_2(s) = \frac{0.304}{s} \quad \frac{(1 + 3.395\,s + 17.48\,s^2)}{1 + h\,s^4}$$

Choosing arbitrarily a value of $h = 1$ the function $g_2(s)$ becomes

$$g_2(s) = \frac{-(1 + 3.1s + 1.5s^2)}{2.5 + 0.9s + \frac{1}{4}\sum_{k=1}^{8} \frac{(1 + 0.2s + s^2)(4a_k s + k\,b_k)}{\frac{k^2}{16} + 0.2s + s^2} \frac{0.304}{s} \left(\frac{1 + 3.395s + 17.48s^2}{1 + s^4} \right) (1.5s + 1.5s^2)}$$

For the condition where $s = i\omega$

$$g_2(i\omega) = \frac{-(1 - 1.5\omega^2 + 3.1i\omega)}{2.5 + 0.9i\omega + \frac{1}{4}\sum_{k=1}^{8} \frac{(1-\omega^2+0.2i\omega)(kb_k+4a_ki\omega)}{\frac{k^2}{16} - \omega^2 + 0.2i\omega} \left| \frac{1.034}{1+\omega^4} - \frac{0.304 - 5.32\omega^2}{\omega(1+\omega^4)} \right| (-1.5\omega^2+1.5i\omega)}$$

This function is plotted on Figure 5 and shows failure to provide complete stability since it cuts through the unit circle.

For a value of $h=10$ however, the function $g_2(i\omega)$ stays clear of the unit circle for small values of ω, as shown on Figure 6 (on this plot also are shown the unstable curves of the motor without feedback and the curve for the approximate behavior of with feedback for small values of ω). As ω increases, $g_2(i\omega)$ moves down toward $-\infty i$; as s traces the arc in the right-half plane shown on Figure 2, $g_2(s)$ proceeds in a large clockwise arc in the left half-plane and returns to the positive imaginary axis and finally traces a mirror image of the contour below the real axis. The closed contour, therefore, does not enclose the unit circle.

To check for unconditional stability the Nyquist criterion must be applied to the denominator of $g_2(s)$, namely $D_2(s) + F_1(s)F_2(s)D_f(s)$. As shown on Figure 7, the plot of this function makes no revolutions around the origin demonstrating unconditional stability for all values of time lag.

Of special interest is the behavior of $g_2(i\omega)$ in the vicinity of $\omega = 0.9$. For frequencies close to this value the proximity of the curve to the unit circle shows that pressure oscillations in the combustion chamber may be poorly damped.

VI. CONCLUDING REMARKS

The scheme of introducing a sampling circuit in the feedback loop to transform the pressure signals in a certain manner and alleviate probable mechanical difficulties in the variable capacitance does not appear to make the problem of designing a stabilizing circuit more difficult than usual. The question now arises as to the possibility of designing a practical sampling circuit with real components that will transform symmetric signals to non-symmetric signals. It is necessary to introduce an actual nonlinear circuit into the problem and to analyze its stability and performance. In all probability the technique of analysis must be modified.

REFERENCES

1. D. F. Gunder and D. R. Friant, "Stability of Flow in a Rocket Motor", J. Appl. Mech. (ASME) Vol. 17, (1950), pp. 327-333.

2. M. Summerfield, "A Theory of Unstable Combustion in Liquid Propellant Rocket Motors", J. American Rocket Society, Vol. 21, (1951), pp. 108-114.

3. L. Crocco, "Aspects of Combustion Stability in Liquid Propellant Rocket Motors", J. American Rocket Society, Vol. 21, (1951), pp. 7-16.

4. Tsien, H. S., "Servo-Stabilization of Combustion in Rocket Motors", J. American Rocket Society, Vol. 22, (1952), pp. 256-263.

5. F. E. Marble and D. W. Cox, "Servo-Stabilization of Low-Frequency Oscillations in a Liquid Bipropellant Rocket Motor", J. American Rocket Society, Vol. 23, (1953), pp. 63-74.

6. M. Satche, "Discussion of a Paper by H. I. Ansoff", J. Appl. Mech. (ASME) Vol. 16, (1949), pp 419-420.

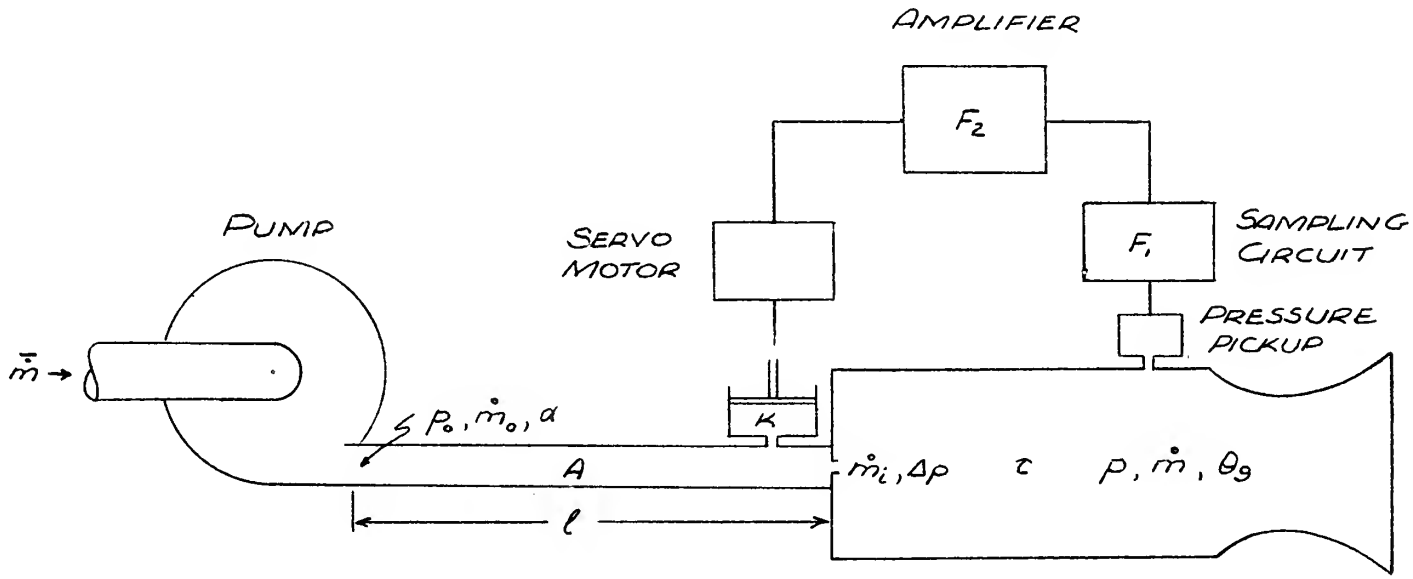

FIGURE 1
ELEMENTS OF A LIQUID MONOPROPELLANT
ROCKET MOTOR WITH FEEDBACK SERVOMECHANISM

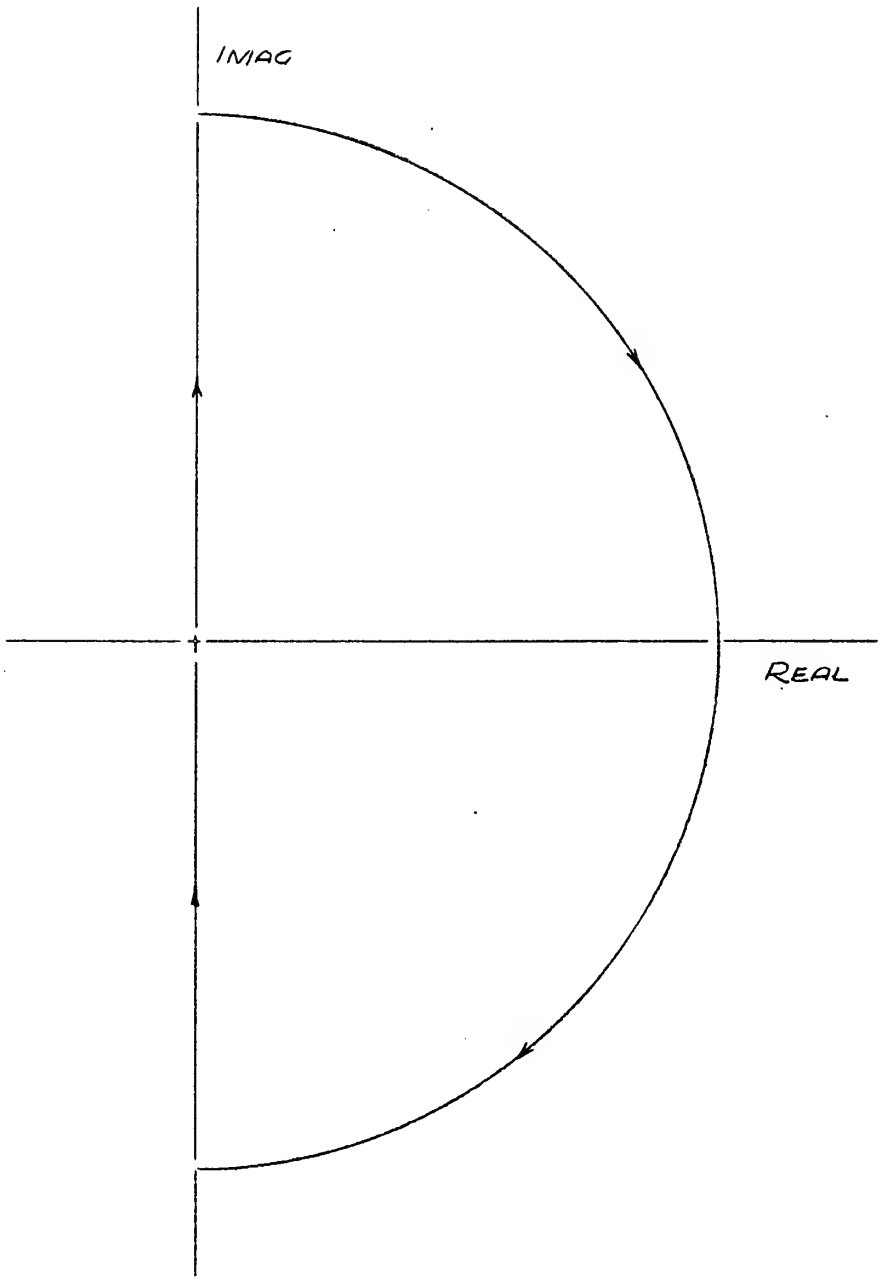

FIGURE 2
CONTOUR OF S IN THE POSITIVE
HALF-PLANE DESCRIBED IN STABILITY ANALYSIS

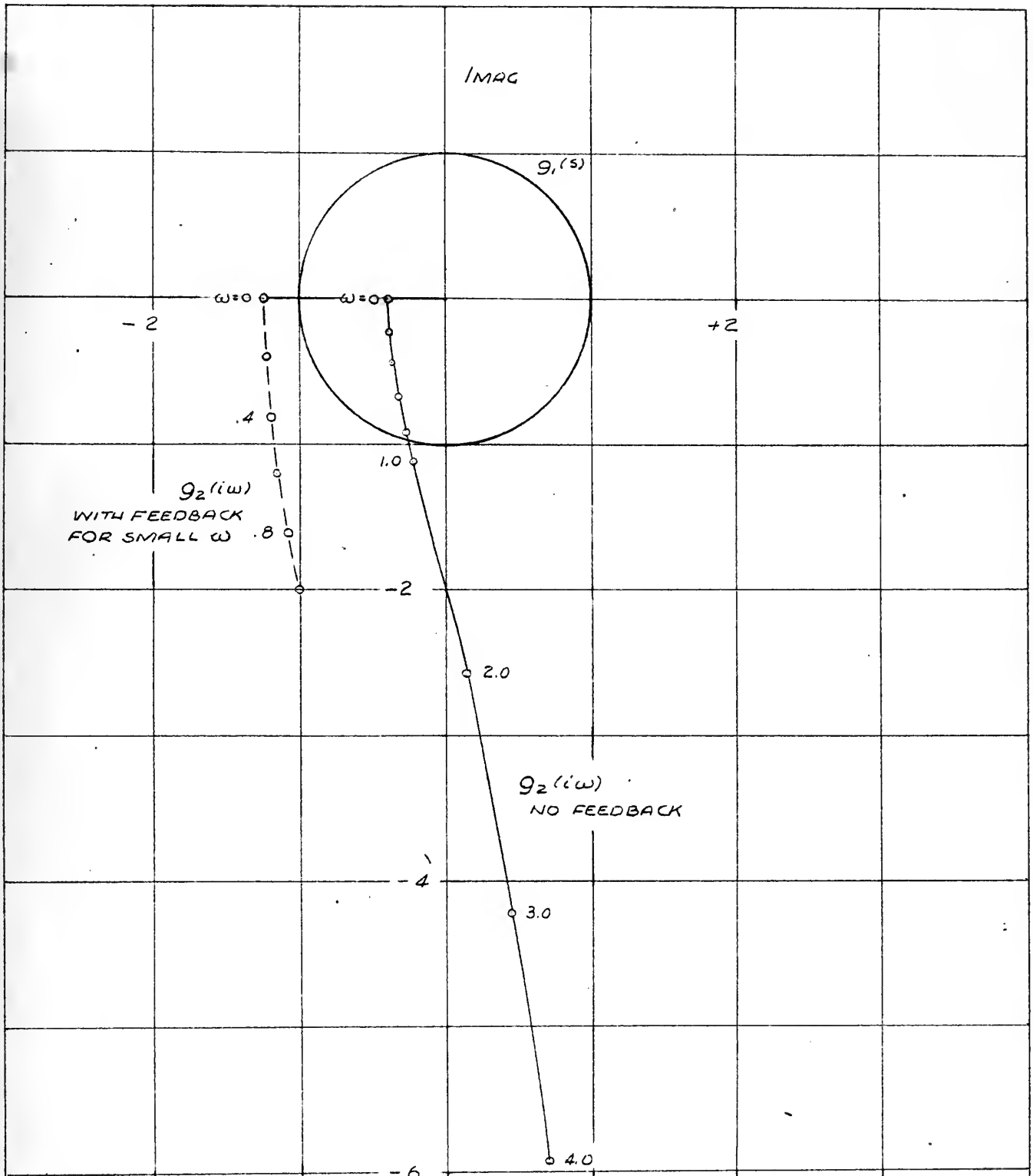

FIGURE 3

SATCHE DIAGRAM FOR ROCKET MOTOR

$\alpha=1.0 \quad P=1.0 \quad J=1.5 \quad n=0.6$

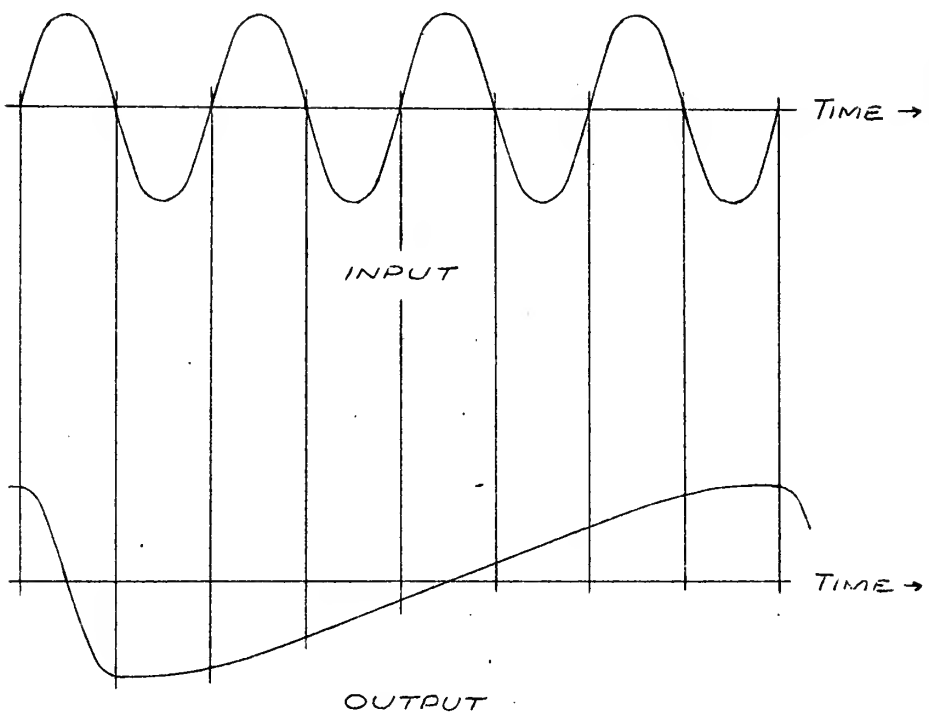

FIGURE 4
SAMPLING CIRCUIT CHARACTERISTICS

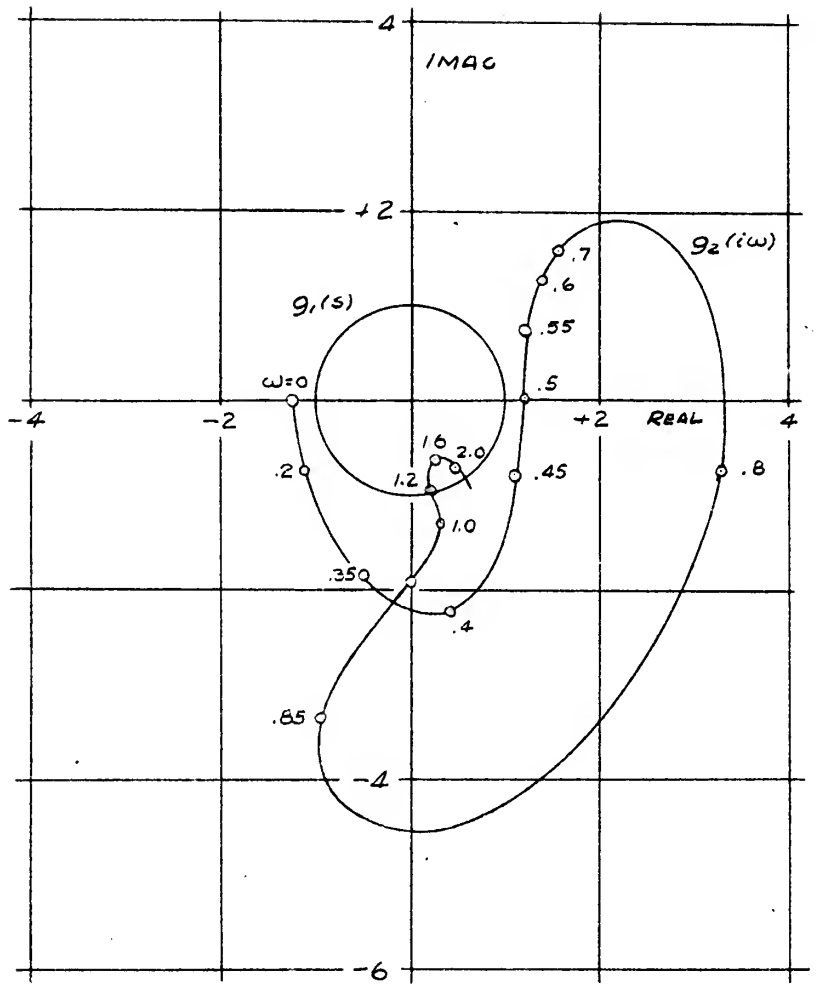

FIGURE 5
SATCHE DIAGRAM FOR ROCKET MOTOR
WITH FEEDBACK
$h = 1$

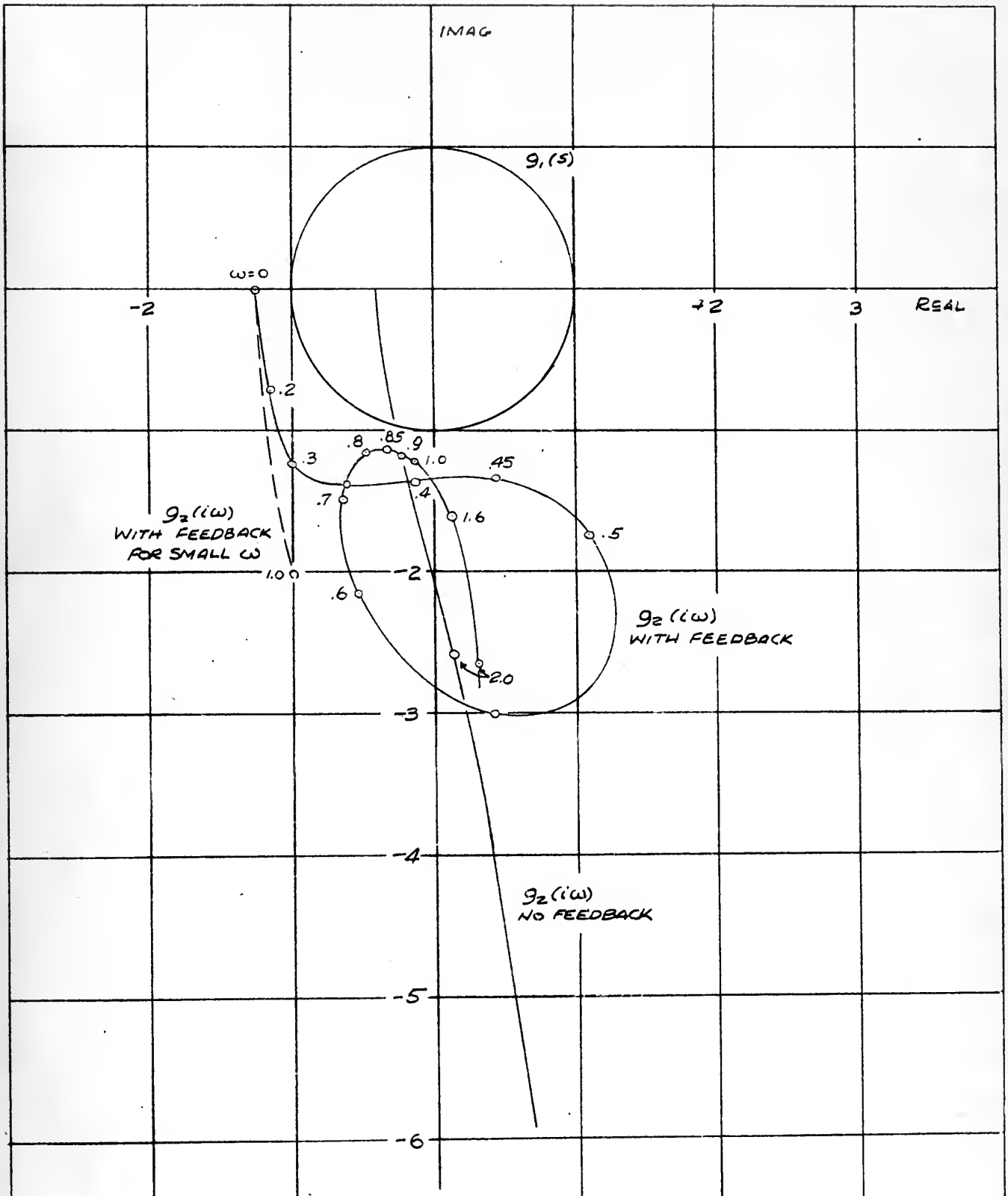

FIGURE 6

SATCHE DIAGRAM FOR ROCKET MOTOR WITH FEEDBACK

$h = 10$

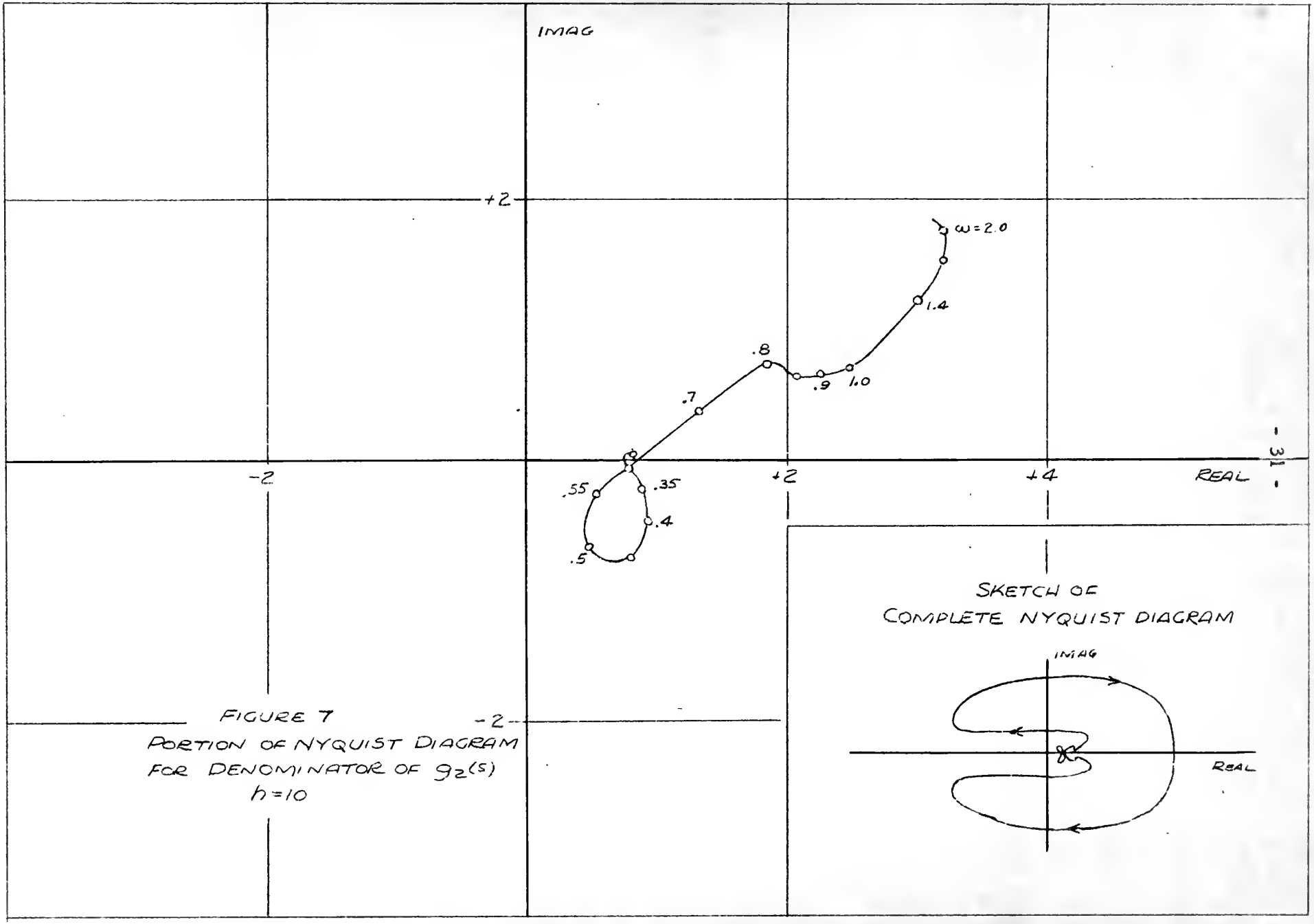

FIGURE 7
PORTION OF NYQUIST DIAGRAM
FOR DENOMINATOR OF $g_2(s)$
$h=10$

SKETCH OF
COMPLETE NYQUIST DIAGRAM